

## Gravity waves above Andes detected from GPS radio occultation temperature profiles: Mountain forcing?

A. de la Torre and P. Alexander

Departamento de Física, Facultad de Ciencias Exactas y Naturales, Universidad de Buenos Aires, Ciudad Universitaria, Buenos Aires, Argentina

Received 11 March 2005; revised 26 July 2005; accepted 1 August 2005; published 15 September 2005.

[1] A significant wave activity in the upper troposphere and lower stratosphere at midlatitudes (30–40S) above the Andes Range was recently detected from Global Positioning System Radio Occultation (GPS RO) temperature profiles, retrieved from SAC-C (Satélite de Aplicaciones Científicas-C) and CHAMP (CHALLENGING Minisatellite Payload) satellites. Previously, large amplitude, long vertical wavelength structures have been reported in this region, as detected from other limb-sounding devices and have been identified as mountain waves (MWs). The capability of GPS RO observations to detect typical MWs with horizontal wavelengths shorter than 150 km, as well as the proper association of the observed wave activity to mountain forcing is put in doubt. Other three possible sources are discussed. In particular, the generation of inertio-gravity waves by geostrophic adjustment near to a permanent jet situated above the mountains, may constitute another important mechanism in this region. These waves may possess longer horizontal and perhaps shorter vertical wavelengths than those typically expected in MWs and could be more easily detected from limb-sounding profiles. The “jet” mechanism will be discussed in a second paper. **Citation:** de la Torre, A., and P. Alexander (2005), Gravity waves above Andes detected from GPS radio occultation temperature profiles: Mountain forcing?, *Geophys. Res. Lett.*, 32, L17815, doi:10.1029/2005GL022959.

### 1. Introduction

[2] It is generally accepted [e.g., *Fritts and Alexander*, 2003, and references therein] that the main gravity wave sources in the lower and middle atmospheres are topography, convection, shear generation, geostrophic adjustment and wave-wave interaction. The observation of wave structures in the lower and middle atmosphere has been performed by means of various ground-based, in situ and spaceborne techniques. Recently, the use of the occultation measurement principle to observe the Earth’s atmosphere and climate exploited solar, lunar, stellar, navigation and satellite-crosslink signals for diverse studies [*Kirchengast*, 2004]. In particular, atmospheric parameters such as temperature, pressure, water vapor and geopotential have been obtained since 2001 from the German and Argentine Low Earth Orbit (LEO) satellites CHAMP and SAC-C, respectively. The simultaneous global coverage, sub-Kelvin temperature accuracy, high vertical resolution, long-term stability and the absence of limitations imposed by weather conditions make this technique unique [see, e.g., *Hajj et al.*,

2004; *Kirchengast*, 2004, and references therein]. Recently, an analysis of global distribution of gravity wave activity in the upper troposphere and lower stratosphere between June 2001 and March 2003 was performed by *de la Torre et al.* [2004a], using temperature profiles retrieved from Global Positioning System Radio Occultation (GPS RO) experiments on board the SAC-C and CHAMP satellites. For vertical wavelengths shorter than 3.5 km, a considerable wave activity in equatorial areas above Indonesia, Brazil and India was mainly observed (well correlated with outgoing longwave radiation) and systematic wave activity enhancements in the winter hemisphere. For vertical wavelengths longer than 3.5 km, particular attention was given to signals above Central Andes, and the possibility to associate them to the presence of mountain waves (MWs) was suggested. Previously, limb viewing satellite data from Cryogenic Infrared Spectrometers and Telescopes for the Atmosphere (CRISTA) were used to state that topography was the source for waves observed in the stratosphere from space [*Eckerman and Preusse*, 1999; *Preusse et al.*, 2002]. At the same time, *McLandress et al.* [2000] and *Jiang et al.* [2002] analyzed Microwave Limb Sounder (MLS) data and concluded that the source giving rise to the strong radiance variances observed above the Andes Range should be the forcing of MWs. A similar conclusion was suggested by *Hocke et al.* [2002] from GPS/MET RO data. In the present work, we discuss the possible observation of MW signatures above Central Andes, as detected from CHAMP and SAC-C RO data.

### 2. GPS RO Data

[3] We subdivided both hemispheres in independent, adjacent cells of 5 per 10 degrees in longitude and latitude respectively. The retrieved temperature  $T$ , previously processed at Jet Propulsion Laboratory (JPL), was splined with a 200 m step (we observed that larger steps did not essentially alter the resulting profiles). Normalized temperature fluctuations  $(T'/T_b)^2$  (relative  $T$  variance) were calculated as follows. The  $T$  profiles were low pass filtered, with a cutoff at 9km, obtaining  $T_b$ . The filter applied is non-recursive and to avoid Gibbs effects a Kaiser window was used. The filter was applied again to the difference  $T - T_b$ , now with a cutoff at 3 km, giving  $T'$  profiles, which isolate wavelengths between 3 and 9 km. Typical mountain waves observed in the region belong to this range [see, e.g., *Eckerman and Preusse*, 1999] and in what follows we constrain ourselves to it. In the data set here considered, bias in the temperature fluctuations greater than 3 K is frequently observed above and below 29 and 8 km respectively, and sometimes even within this range. Our

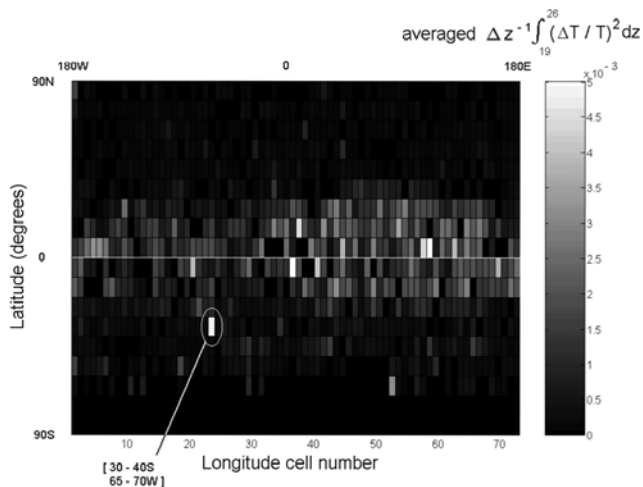


**Figure 1.** Longitude-latitude view of the relative temperature variance  $(T'/T_b)^2$ , integrated between 19 and 26 km height and averaged for all the events detected during August 2001.  $\Delta z = 7$  km (reproduced with kind permission of Springer Science and Business Media from Figure 2 of *de la Torre et al.* [2005]).

main interest is here the upper troposphere and lower stratosphere regions, thus we restrict to the altitude interval 10–27 km.

[4] Considerably intense signatures of wave activity with respect to non-equatorial regions in the southern hemisphere were detected in the region 70–65W and 30–40S, in Argentina, at the eastern side of the highest Andes Mountains (tops around 7 km). Figure 1 shows a longitude-latitude view of  $(T'/T_b)^2$ , integrated between two altitude levels (relative  $T$  variance content) in the lower stratosphere (19 and 26 km), averaged during August 2001. This may be considered a measure of mean gravity wave energy activity there [*Hocke et al.*, 2002]. A clear enhancement near to the Andes is seen, pointed out within the oval.

[5] The capability of GPS-LEO RO observations to detect short horizontal wavelength MWs should be now evaluated. The vertical resolution available from this technique depends on different factors: large vertical refractivity gradients, measurement precision, inversion scheme and diffraction limit, and may be roughly stated between .8 and 1.0 km [e.g., *Kursinski et al.*, 1997]. Recent works [*Steiner and Kirchengast*, 2000; *Tsuda and Hocke*, 2002; *Marquardt and Healy*, 2004] show that for vertical wavelengths smaller than 2 km the identification of waves may depend on the retrieval used, particularly the applied filtering. If a sounding path was vertically directed, as it would be the case during a zero background horizontal wind radiosounding, no restrictions would limit the detection of usual large amplitude structures with vertical wavelengths longer than 2 km. Accordingly, currently observed large amplitude waves, with intrinsic frequencies between inertial and buoyancy limits could be detected. However, the available resolution due to smearing effect along the line-of-sight (LOS) during the occultation event is of the order of the horizontal resolution itself, and limited to around 150 km (cross LOS the horizontal resolution is an order of magnitude better). Depending on the angle between the LOS and the wave vector, the wave signal detected and the resolution

attained may become even worse [*Jiang et al.*, 2002]. These aspects should prevent for the observation of short horizontal wavelengths, as those generated by mountains, unless in the horizontal plane the wavefronts are slightly slanted with respect to the LOS. Therefore, GPS RO vertical profiles might include gravity waves with small horizontal wavelengths in very particular cases. The wave activity calculated from  $T$  variances as well as any gravity wave climatology from GPS RO data may probably in general be underestimated. Another consideration to be taken into account, which mostly affects medium-scale waves with horizontal to vertical wavelength ratios less than 100, is the assumed spherical symmetry during the retrieval process, which may produce a significant phase shift of a given perturbation during the inversion and a significant bias in the retrieved  $T$  profile [*Belloul and Hauchecorne*, 1997].

### 3. Analysis

[6] From the almost 150,000 RO events globally retrieved between June 1, 2001 and March 31, 2003, a subset of 89

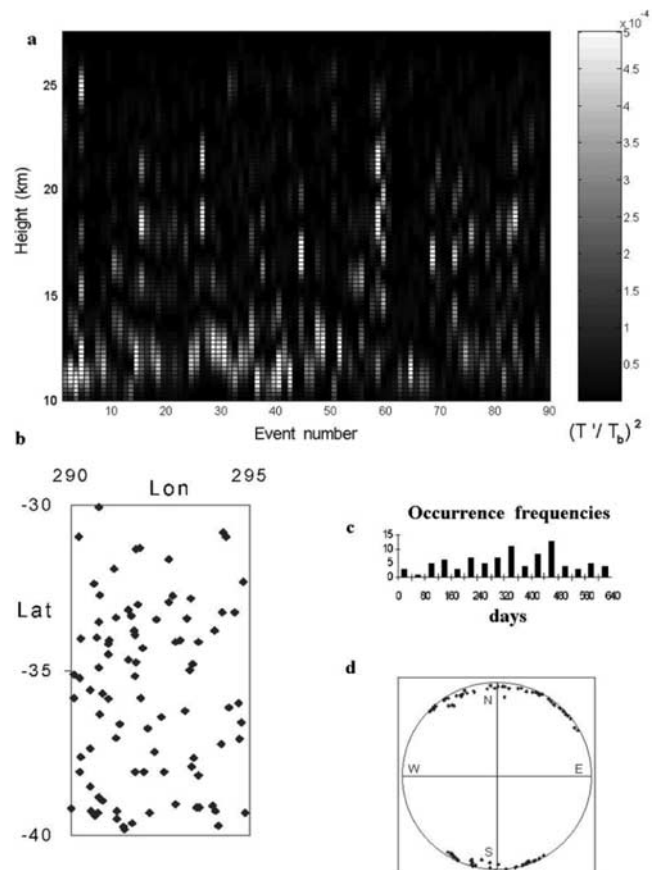


**Figure 2.** (a)  $T$  relative variance of 89 events detected within 70–65W and 30–40S, retrieved between June 1, 2001 and March 31, 2003, as a function of height, chronologically ordered in the horizontal axis. (b) Geographic distribution of the RO events shown in Figure 2a. (c) Occurrence frequency in 40 days intervals of the RO events shown in Figure 2a, which comprise 639 days. (d) The projection on the horizontal plane of the unit vector associated to the RO sounding direction for each of the events shown in Figure 2a.

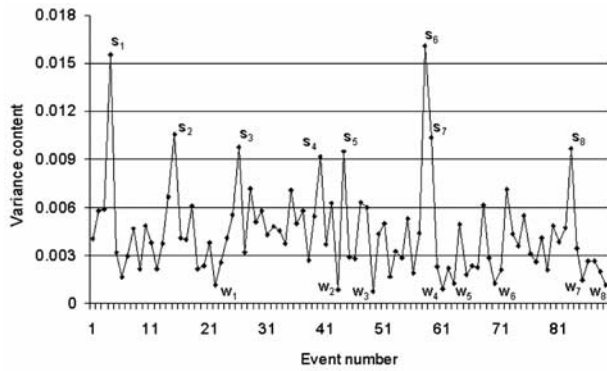


**Figure 3.** Relative  $T$  variance content between 10 and 27 km height, for the 89 RO events presented in Figure 2a.

of them fell within 70–65W and 30–40S. In Figure 2a, the  $T$  relative variance of these events, chronologically ordered in the horizontal axis, is shown as a function of height. Each event is represented by a single vertical column between 10 and 27 km height, and a horizontal width of one pixel. The vertical extension of each pixel equals the spline step of 200 m chosen. Alternate enhancements and depressions of wave activity may be observed, and the distance between two consecutive maxima corresponds to half a vertical wavelength. Some features can be remarked in Figure 2a: i) From the relative intensity of wave activity, “stronger” and “weaker” events may be distinguished; ii) a predominant apparent vertical wavelength, situated between 5 and 6 km is clear; iii) the altitude values corresponding to minima around 15.0, 17.5 and 20.0 km appear slightly displaced among events. Plots belonging to adjacent cells (70–65W, 40–50S and 20–30S, not shown here) exhibit wave activity similar to that seen in Figure 2a. In Figures 2b and 2c, the uneven geographic and time distribution of the 89 events presented in Figure 2a may be seen. In Figure 2d we exhibit the directions that the 89 ROs point at. They have a low elevation angle and always differ significantly from the west-east direction, which is caused by the particular configuration of the satellites. Due to the North-South direction of the Andes Mountains at these latitudes, where their orographic structure is basically dependent on the height and the longitude, wavefronts are theoretically expected to be roughly parallel to the Andes Range [Baines, 1995]. According to the horizontal resolution of the measuring technique this places a scenario where short horizontal wavelengths might be seen. In reference to Figure 2a, as 3D limb sounding paths are directed far away from the vertical, the slope effect of phase surfaces introduces a systematic discrepancy between “real” and “apparent” (detected) vertical wavelengths (there is no additional displacement effect because the duration of each occultation event is very short). This effect will be more or less significant, depending on the angle of phase surfaces of the wave structures observed [de la Torre and Alexander, 1995]. In particular, this difference is expected to be greater for MWs than for inertio-gravity waves (almost horizontal phase surfaces). In Figure 3, the relative  $T$  variance content between 10 and 27 km is shown. Two intense events emerge and a total of 8 strong events,

denoted with “s”, have been differentiated. For comparison, we marked also the 8 weakest events (denoted with “w”).

[7] We should note that the region under discussion represents a natural laboratory where a simultaneous competition between at least 4 different typical sources of gravity wave generation must be identified and distinguished. Possible selection mechanisms of wave propagation into the lower and middle atmosphere should be expected to be associated to these sources. There is an obvious possible link of the observed wave activity with the direct forcing of the Andes Range (keeping in mind that still an important short-scale orographic contribution may remain invisible to RO GPS data). However, we also observed that a westerly jet is permanently situated above Central Andes, centered around 30S, and subject to a repeated annual variability, so inertio-gravity waves could be generated near to it. As it is known, they are generated when mass and momentum are redistributed so as to ultimately achieve geostrophic balance from an initially unbalanced state [Blumen, 1972; Uccellini and Koch, 1987]. Two remaining significant sources of gravity waves in the region must be considered: i) deep convection, mainly between October and March and strongly subject to local atmospheric conditions [see, e.g., de la Torre et al., 2004b], and ii) vertical shear wind generation.

[8] The enhancements observed might correspond to MWs, taking into account the expected strong orographic forcing at these latitudes, where the highest Andes Mountains are found. Let us investigate the strongest case, observed on August 30, 2001. For steady forcing of a stratified fluid, such as flow over orography, the Scorer parameter  $L^2$  is defined by  $L^2 = (N(z)^2/U(z)^2) - U_{zz}/U$ , where  $N$ ,  $U$  and  $U_{zz}$  are the buoyancy frequency, the wind in the direction of wave propagation and its second derivative with respect to the height  $z$ , respectively [see, e.g., Baines, 1995]. For propagating waves, we know that the relation  $(2\pi/\lambda_v)^2 = L^2 - (2\pi/\lambda)^2 > 0$  must be verified, where  $\lambda_v$  and  $\lambda$  are the vertical and horizontal wavelengths. As stated above the wavefronts of possible MWs generated in the region are mainly parallel to Andes, but the minimum  $L$  value required for non-trapped modes was anyway estimated for leewards wave directions between North and South every 15 degrees, using data obtained from NCEP reanalyses. From Figure 4 we conclude that on August 30, 2001, free

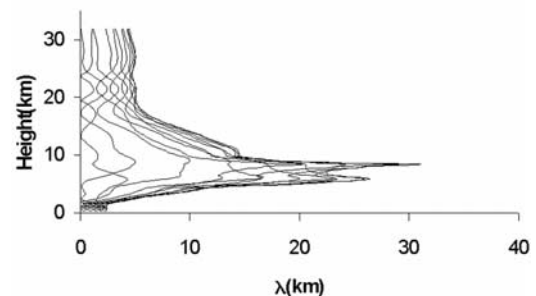


**Figure 4.** The calculated minimum horizontal wavelengths allowed to propagate for leewards directions between North and South at steps of 15 degrees vs. height, using data obtained from NCEP reanalyses on August 30, 2001 at 6:00 am.

propagation was expected for orographically generated horizontal wavelengths longer than 30 km. Indeed, this does not represent a severe restriction for typical MWs [see, e.g. *Fritts and Alexander, 2003*]. In addition, MWs seem here free to propagate from the troposphere to the lower stratosphere, as from NCEP horizontal wind data no critical levels appear against MWs (zero mean wind or considerable veering of mean wind with altitude). On the other hand, we observed a very low correlation between mean low level westerlies at the West of the Andes Range (at 925, 850 and 700 mbars) and wave activity (represented by the relative  $T$  variance content) for the 89 RO events shown in Figure 3.

[9] The importance of the generation of inertio-gravity waves near to the jet by geostrophic adjustment, with longer horizontal and perhaps shorter vertical wavelengths than those expected for MWs, is considered in a manuscript in preparation. These waves could be more easily detected from GPS-RO profiles than MWs. From cloud top temperature imagery, no correspondence was detected between the strong events and deep convection processes in the lower atmosphere. Five of them (08/30/01, 05/22/02, 06/04/02, 09/09/02 and 09/11/02) occurred clearly outside of the usual period of severe convection in the region considered, while the other three (11/20/01, 03/07/02 and 02/01/03) were observed within. The vertical wind shear associated with the jet is a possible wave source through shear instabilities, where the Richardson number  $Ri$  be less than 25. We are not able to accurately test this parameter from NCEP reanalyses data, but the horizontal wavelengths expected at least theoretically for this mechanism are well below 150 km [*Lalas and Einaudi, 1976*].

#### 4. Conclusions

[10] From GPS RO temperature profiles retrieved from SAC-C and CHAMP satellites, large amplitude, long vertical wavelength structures revealing more intense wave activity than in any other non-equatorial region in the southern hemisphere was detected between 70–65W and 30–40S, in Argentina, at the eastern side of the highest Andes Mountains. The capability of these observations to detect typical MWs with horizontal wavelengths shorter than the horizontal resolution along LOS (150 km), may depend during each RO event on the angle between LOS and the wave phase surfaces to be detected. The observed wave activity exhibits in the studied region a very low correlation with forcing by low level westerlies. From the other three significant gravity wave sources usually present in the region, a permanent jet observed below the tropopause may be more important than deep convection and shear instabilities, through the generation of long horizontal wavelength inertio-gravity waves during geostrophic adjustment processes.

[11] **Acknowledgments.** Manuscript prepared under grants UBA X021 and CONICET PEI 6373. Both authors are members of CONICET. We acknowledge data provided by the NOAA-CIRES/Climate Diagnostics

Center, Boulder (CO) from their website [www.cdc.noaa.gov](http://www.cdc.noaa.gov). We thank both referees for very helpful comments.

#### References

- Baines, P. G. (1995), *Topographic Effects in Stratified Fluids*, 482 pp., Cambridge Univ. Press, New York.
- Belloul, M. B., and A. Hauchecorne (1997), Effect of periodic horizontal gradients on the retrieval of atmospheric profiles from occultation measurements, *Radio Sci.*, *32*, 469–478.
- Blumen, W. (1972), Geostrophic adjustment, *Rev. Geophys.*, *10*, 485–528.
- de la Torre, A., and P. Alexander (1995), The interpretation of wavelengths and periods as measured from atmospheric balloons, *J. Appl. Meteorol.*, *34*, 2747–2754.
- de la Torre, A., T. Tsuda, G. Hajj, and J. Wickert (2004a), A global distribution of the stratospheric gravity wave activity from GPS occultation profiles with SAC-C and CHAMP, *J. Meteorol. Soc. Jpn.*, *82*, 407–417.
- de la Torre, A., D. Vincent, R. Tailleux, and H. Teitelbaum (2004b), A deep convection event above the Tunuyán Valley near to the Andes Mountains, *Mon. Weather Rev.*, *132*, 2259–2268.
- de la Torre, A., T. Tsuda, H. F. Tsai, G. Hajj, and J. Wickert (2005), Analysis of gravity wave variability from SAC-C and CHAMP occultation profiles between June 2001 and March 2003, in *Earth Observation With CHAMP: Results From Three Years in Orbit*, pp. 609–614, Springer, New York.
- Eckermann, S. D., and P. Preusse (1999), Global measurements of stratospheric mountain waves from space, *Science*, *286*, 1534–1537.
- Fritts, D. C., and J. Alexander (2003), Gravity wave dynamics and effects in the middle atmosphere, *Rev. Geophys.*, *41*(1), 1003, doi:10.1029/2001RG000106.
- Hajj, G. A., et al. (2004), CHAMP and SAC-C atmospheric occultation results and intercomparisons, *J. Geophys. Res.*, *109*, D06109, doi:10.1029/2003JD003909.
- Hocke, K., T. Tsuda, and A. de la Torre (2002), A study of stratospheric GW fluctuations and sporadic E at midlatitudes with focus on possible orographic effect of Andes, *J. Geophys. Res.*, *107*(D20), 4428, doi:10.1029/2001JD001330.
- Jiang, H. J., D. L. Wu, and S. D. Eckerman (2002), Upper Atmosphere Research Satellite (UARS) MLS observation of mountain waves over the Andes, *J. Geophys. Res.*, *107*(D20), 8273, doi:10.1029/2002JD002091.
- Kirchengast, G. (2004), Occultations for probing atmosphere and climate: Setting the scene, in *Occultations for Probing Atmosphere and Climate*, pp. 1–8, Springer, New York.
- Kursinski, E. R., et al. (1997), Observing Earth's atmosphere with radio occultation measurement using the Global Positioning System, *J. Geophys. Res.*, *102*, 23,429–23,465.
- Lalas, D. P., and F. Einaudi (1976), On characteristics of gravity waves generated by atmospheric shear layers, *J. Atmos. Sci.*, *33*, 1248–1259.
- Marquardt, C., and S. Healy (2004), Measurement noise and stratospheric gravity wave characteristics obtained from GPS occultation data, *Forecasting Res. Tech. Rep. 448*, 17 pp., U. K. Meteorol. Off., Exeter.
- McLandress, C., M. J. Alexander, and D. L. Wu (2000), Microwave Limb Sounder observations of gravity waves in the stratosphere: A climatology and interpretation, *J. Geophys. Res.*, *105*, 11,947–11,967.
- Preusse, P. A., et al. (2002), Space-based measurements of stratospheric mountain waves by CRISTA: 1. Sensitivity, analysis method and a case study, *J. Geophys. Res.*, *107*(D23), 8178, doi:10.1029/2001JD000699.
- Steiner, A. K., and G. Kirchengast (2000), Gravity wave spectra from GPS/MET occultation observations, *J. Atmos. Oceanic Technol.*, *17*, 495–503.
- Tsuda, T., and K. Hocke (2002), Vertical wave number spectrum of temperature fluctuations in the stratosphere using GPS occultation data, *J. Meteorol. Soc. Jpn.*, *80*, 925–938.
- Uccellini, L. W., and S. E. Koch (1987), The synoptic settings and possible energy sources for mesoscale wave disturbances, *Mon. Weather Rev.*, *115*, 721–729.

P. Alexander and A. de la Torre, Departamento de Física, Facultad de Ciencias Exactas y Naturales, Universidad de Buenos Aires, Ciudad Universitaria, 1428 Buenos Aires, Argentina. (peter@df.uba.ar; delatorr@df.uba.ar)